Role of 18-Crown-6 and 15-Crown-5 Ethers in the Crystallization of Polytype Faujasite Zeolites

Eddy J. P. Feijen,* Koenraad De Vadder, Marleen H. Bosschaerts, Jan L. Lievens, Johan A. Martens, Piet J. Grobet, and Pierre A. Jacobs

Contribution from the Centrum voor Oppervlaktechemie en Katalyse, KU Leuven, Kardinaal Mercierlaan 92, B-3001 Heverlee (Leuven), Belgium

*Received October 12, 1993**

Abstract: Phases obtained during crystallization of the cubic and the hexagonal end-member of the family of faujasite polytype zeolites and of their intergrowths from aluminosilicate hydrogels containing 15-crown-5 ether, 18-crown-6 ether, or a mixture of these ethers were characterized by XRD, IR, SEM, ^{29}Si and ^{13}C MAS NMR, TGA, and nitrogen adsorption. The siting of crown ethers in the intracrystalline voids of the zeolites is derived from TGA and nitrogen adsorption data. The EMT content of FAU/EMT intergrowths is determined by multiphase Rietveld refinement of XRD patterns. Correlations between gel composition, crystallization kinetics, and EMT content of end products are established. A molecular model for crystallization consistent with the observed correlations is proposed.

Introduction

Attempts to unravel the synthesis mechanism of faujasite-type zeolites and molecular sieves and to determine factors that direct zeolite crystallization to one of the polytype faujasite materials remain very timely, because of their high potential for e.g. catalysis,[1,2] separation purposes,[3] supramolecular catalysis[4] and nanochemistry,[5] photochemistry,[6] and electrochemistry.[7,8] To these materials belong pure structure types characterized by the IUPAC codes EMT and FAU,[9] inter- and overgrowths combining varying amounts of both structure types.[10-16]

The synthesis of a pure EMT phase was accomplished for the first time by Delprato et al., starting from an aluminosilicate hydrogen containing 18-crown-6 ether.[17] The replacement of 18-crown-6 by 15-crown-5 ether leads to the crystallization of the cubic end-member, having FAU topology.[17] Formally, both structure types can be built from truncated octahedra, often called "sodalite units" or cubo-octahedra, which are linked together through hexagonal prisms, thus giving rise to faujasite sheets (Figure 1). Due to the different linking of sodalite cages, the micropore structures of the EMT and FAU frameworks are substantially different.[18] In FAU, the largest void spaces are called "supercages". Supercages have a diameter of 1.3 nm and are accessible through four circular 12-ring windows with a free dimension of 0.74 nm. In EMT, an equal number of two different types of large cages is present, conveniently denoted as hypocages and hypercages.[19] Hypercages have free dimensions of 1.3 × 1.3 × 1.4 nm and are accessed through two circular apertures similar to those of supercages and three apertures of elliptic shape with free diameters of 0.69 × 0.74 nm.[18] The hypocages have free dimensions of 0.69 × 1.3 × 1.3 nm and can be entered through three elliptic windows.[18]

A number of zeolites with aluminosilicate composition have been identified as structural mixtures of FAU and EMT. ZSM-2,[20,21] ZSM-3,[10] ZSM-20,[12] CSZ-1,[22,23] ECR-30,[13] and ECR-35[15] are structural composites containing various amounts of FAU and EMT in a variety of spacial arrangements. Intergrown FAU-EMT phases can also be obtained from synthesis mixtures containing a mixture of 18-crown-6 and 15-crown-5 ether.[14,24] Although these products have been considered originally as overgrowths,[16] their intergrown nature has later been confirmed using high-resolution electron microscopy.[14,25]

On the basis of consistent data on nucleation and crystal growth kinetics, critical gel compositional parameters, and EMT contents of intergrowths, a crystallization model is presently derived for the molecular assembling of crown ether molecules and layers of linked supercages into FAU and EMT aluminosilicate frameworks or their intergrowths. The siting of the crown ether molecules in the cages of the growing crystals is used to rationalize the nature of the materials obtained.

Experimental Section

Materials. Hydrogels with the compositions specified in Table 1 were prepared using the following reagents: Ludox HS-40 (Du Pont), NaOH pellets (Merck), Gibbsite (Fluka), sodium aluminate (Riedel de Hahn), 1,4,7,10,13-pentaoxacyclopentadecane (Janssen Chimica), denoted further as 15-crown-5 ether, 1,4,7,10,13,16-hexaoxacyclooctadecane (Janssen

* Abstract published in *Advance ACS Abstracts,* March 1, 1994.

(1) Venuto, P. B.; Landis, P. S. *Adv. Catal.* **1968**, *18*, 259–365.
(2) Maxwell, I. E. *Adv. Catal.* **1982**, *31*, 1–76.
(3) Coe, C. G. *Gas Separation Technology*; Vansant, E. F., Dewolfs, R., Ed.; Elsevier: Amsterdam, 1990; pp 149.
(4) Parton, R.; De Vos, D.; Jacobs, P. A. *NATO ASI Series, C352*; Derouane, E. G., Lemos, F., Naccache, C., Ribeiro, F. R., Eds.; Kluwer: Dordrecht, The Netherlands, 1992; pp 555–578.
(5) Ozin, G. A.; Gil, G. *Chem. Rev.* **1989**, *89*, 1749–1764.
(6) Suib, S. L. *Chem. Rev.* **1993**, *93*, 803–826.
(7) Davis, M. E. *Acc. Chem. Res.* **1993**, *26*, 111–115.
(8) Davis, M. E.; Lobo, R. L. *Chem. Mater.* **1992**, *4*, 756–768.
(9) Meier, W. M.; Olson, D. H. *Atlas of Zeolite Structure Types*; Butterworths-Heinemann: Surrey, U. K., 1992; pp 88 and ibidem pp 96.
(10) Kokotailo, G. T.; Ciric, J. *Adv. Chem. Ser.* **1971**, *101*, 109–121.
(11) Barrett, M. G.; Vaughan, D. E. W. U.S. Patent 4,309,313, **1982**.
(12) Newsam, J. M.; Treacy, M. M. J.; Vaughan, D. E. W.; Strohmaier, K. G.; Mortier, W. J. *J. Chem. Soc., Chem. Commun.* **1989**, 493–495.
(13) Vaughan, D. E. W. Eur. Patent Appl. 315,461, **1989**.
(14) Anderson, M. W.; Pachis, K. S.; Prébin, F.; Carr, S. W.; Terasaki, O.; Ohsuna, T.; Alfreddson, V. *J. Chem. Soc., Chem. Commun.* **1991**, 1660–1664.
(15) Vaughan, D. E. W.; Strohmaier, K. G.; Treacy, M. M. J.; Newsam, J. M. U.S. Patent 5,116,590, **1992**.
(16) Dougnier, F.; Patarin, J.; Guth, J. L.; Anglerot, D. *Zeolites* **1992**, *12*, 160–166.
(17) Delprato, F.; Delmotte, L.; Guth, J. L.; Huve, L. *Zeolites* **1990**, *10*, 546–552. ECR-30 was originally claimed to be pure EMT.[13] Comparison of XRD patterns indicates that it is closely related to ZSM-20,[34a] which was proven to be "mixed cubic and hexagonal stackings of faujasite sheets".[12]
(18) Thomas, J. M.; Ramdas, S.; Millward, G. R.; Klinowski, J.; Audier, M.; Gonzalez-Calbet, J.; Fyfe, C. A. *J. Solid State Chem.* **1982**, *45*, 368–380.
(19) Martens, J. A.; Jacobs, P. A.; Cartlidge, S. *Zeolites* **1989**, *9*, 423–427.
(20) Barrer, R. M.; Sieber, W. *J. Chem. Soc., Dalton Trans.* **1976**, 1020–1026.
(21) Martens, J. A.; Xiong, Y. L.; Feijen, E. J. P.; Grobet, P. J.; Jacobs, P. A. *J. Phys. Chem.* **1993**, 5132–5135.
(22) Cotterman, R. L.; Hickson, D. A.; Cartlidge, S.; Dybowski, C.; Tsiao, C.; Venero, A. F. *Zeolites* **1991**, *11*, 27–34.
(23) Cartlidge, S.; Nissen, H.-U.; Shatlock, M. P.; Wessicken, R. *Zeolites* **1992**, *12*, 889–897.
(24) Burkett, S. L.; Davis, M. E. *Microporous Mater.* **1993**, *1*, 265–282.
(25) Terasaki, O.; Ohsuna, T.; Alfredsson, V.; Bovin, J.-O.; Watanabe, D.; Carr, S. W.; Anderson, M. W. *Chem. Mater.* **1993**, *5*, 452–458.

0002-7863/94/1516-2950$04.50/0

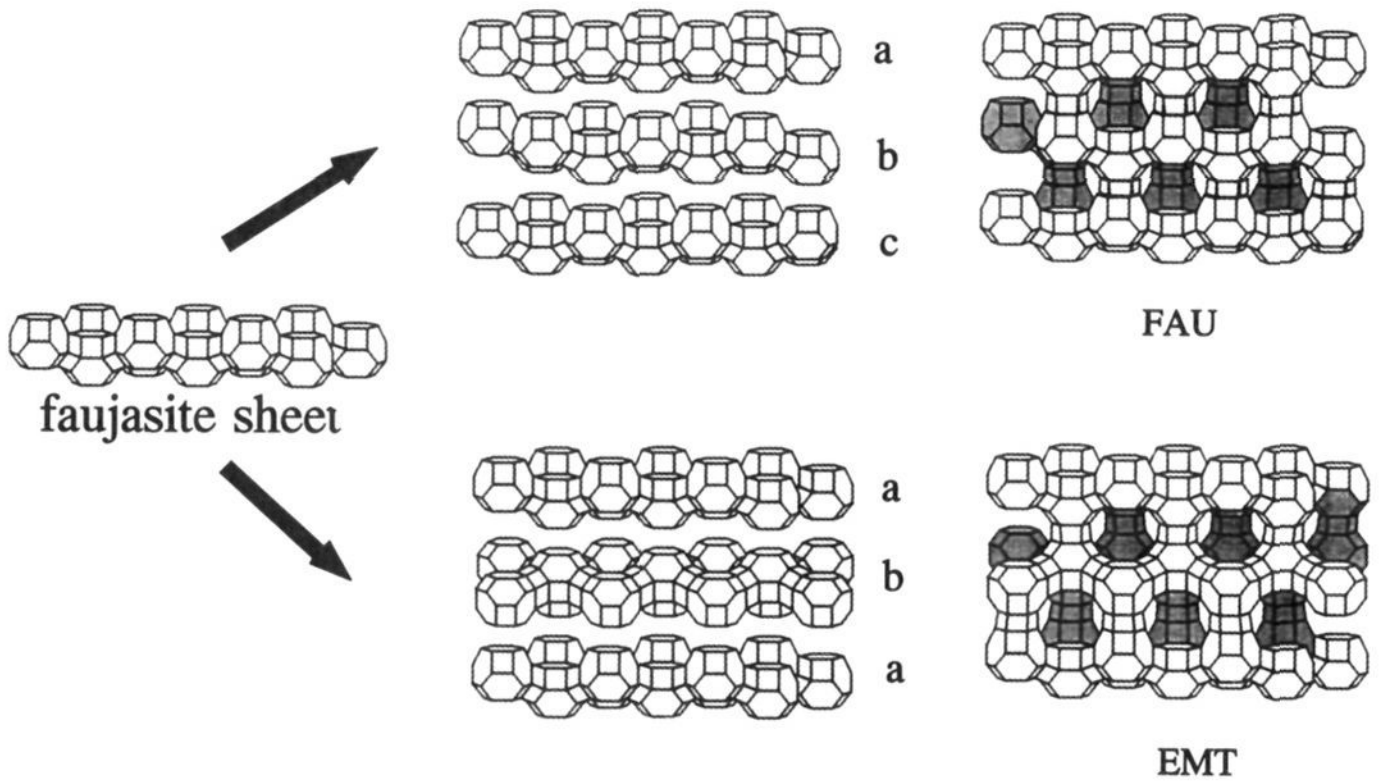

Figure 1. Sheet of cubo-octahedra interconnected via hexagonal prisms, denoted as a faujasite sheet; assembly of faujasite sheets situated on inequivalent positions (a, b, or c) results in the FAU (abc) or EMT (aba) topology.

Table 1. Hydrogel Composition and Nature of Crystalline Phases Obtained after 9 days of Crystallization

	10 SiO_2; Al_2O_3; x Na_2O; y 15-crown-5; z 18-crown-6; 135 H_2O[a]						
sample notation	x	y	z	crown ether/ Na_2O	Na_2O/ SiO_2	OH^-/ SiO_2	phase
FAU-0	2.40	0.00	0.00	0.000	0.240	0.48	FAU
FAU-15	2.40	0.97	0.00	0.405	0.240	0.48	FAU
EMT-18	2.40	0.00	0.97	0.405	0.240	0.48	EMT
FAU-18 a	3.00	0.00	0.97	0.324	0.300	0.60	FAU
FAU-18 b	3.75	0.00	0.97	0.258	0.375	0.75	FAU
FAU-18 c	3.75	0.00	1.52	0.405	0.375	0.75	FAU
FAU-18 d	3.40	0.00	0.97	0.285	0.340	0.48	FAU
MIX 60/40	2.40	0.57	0.40	0.405	0.240	0.48	FAU
MIX 40/60	2.40	0.40	0.57	0.405	0.240	0.48	FAU/EMT
MIX 25/75	2.40	0.25	0.72	0.405	0.240	0.48	FAU/EMT
MIX 20/80	2.40	0.19	0.78	0.405	0.240	0.48	FAU/EMT
MIX 15/85	2.40	0.14	0.83	0.405	0.240	0.48	FAU/EMT
MIX 10/90	2.40	0.10	0.87	0.405	0.240	0.48	FAU/EMT

[a] Molar composition.

Chimica), denoted as 18-crown-6 ether, and deionized water. The crown ether was added to the colloidal silica, diluted with water. Gibbsite was dissolved in an aqueous solution of NaOH under heating at 353 K. The latter solution and the silica sol were combined and stirred for 10 min. The resulting gel was aged at 293 K for 3 days. The aged gel was subsequently transferred into Teflon-lined autoclaves with a capacity of 40 mL and heated at 372 K. After the crystallization time had elapsed, the autoclave was cooled in water. The solids in the autoclave were recovered by filtration, thoroughly washed with deionized water, and dried at 333 K. Final calcination of the solid was done in a muffle furnace at 823 K for 20 h.

The sample notation refers to the crystallographic nature of the phase (FAU for cubic faujasite, EMT for the hexagonal phase, and MIX for a FAU/EMT intergrowth), followed by the nature of the template (0, no template used; 18, 18-crown-6; 15, 15-crown-5) in case of pure phases or by the molar ratio of 15-crown-5/18-crown-6 in case of intergrown phases (MIX). Only sample MIX 60/40, synthesized in excess 15-crown-5, is a pure faujasite.

Methods. X-ray diffraction patterns were recorded with a Philips PW 1050/25 goniometer, equipped with a PW 1965/20 proportional counter. For the Rietveld refinements of the intergrowths, an automated Seifert-Scintag PAD II powder X-ray diffractometer equipped with a proportional counter and a HDK (Seifert) high-temperature camera was used. Calcined samples were evacuated first at 293 K under high vacuum (1 mPa). Subsequently, the temperature was increased at 1 K/min to 673 K and kept at that temperature for at least 12 h. The XRD profiles were recorded at 673 K in vacuum (1 mPa) at steps of 0.01 2θ values. Random noise was reduced by treating the profiles with a digital filter. The profiles were refined using the DBW3.2S (1981) program of Wiles and Young.[26] A detailed description of this pattern-decomposition method and of the refinement strategy used is given in ref 27. Atomic coordinates for EMT and FAU were taken from ref 27 and were not altered in order to keep the ratio parameters/observations acceptable. This however does not substantially influence the scale factors of the individual EMT and FAU phases. For the quantification of the FAU and EMT content in the intergrowths, the method of Hill et al.[28] was used given the severe overlap of diffraction lines.

Thermogravimetric analyses (TGA) and differential thermal analyses (DTA) profiles were recorded on a Setaram TGA 92 thermobalance in oxygen/helium (20/80 v/v) atmosphere using typically 30 mg of sample and a flow of 35 mL/min. The temperature was increased at a rate of 10 K/min from 293 to 823 K.

The NMR measurements were performed using a Bruker 400 MSL spectrometer with a magnetic field of 9.4 T. The ^{29}Si MAS NMR experiments were run at 79.5 MHz, with a pulse length of 4 μs, a pulse interval of 5 s, a spinning rate of 4 kHz, and a number of 11 000 scans. ^{13}C CP MAS NMR spectra were recorded at a frequency of 100.577 MHz, a pulse width of 3 μs, an interval of 5 s, a contact time of 2.5 ms, and a spinning rate of 13 kHz. The ^{13}C chemical shifts are reported relative to Me_4Si.

Infrared spectra were recorded with a Nicolet 730 FTIR spectrometer using the KBr pellet technique.

Scanning electron micrographs were obtained using a Jeol superprobe 733 instrument.

Nitrogen adsorption isotherms at 77 K were recorded using an Omnisorp-100 analyzer from Coulter, operating in the continuous gas introduction and continuous pressure monitoring mode. Using this technique, accurate nitrogen adsorption isotherms were obtained at partial pressures down to 0.1 Pa. Before the nitrogen adsorption isotherms were recorded, calcined samples were outgassed at 673 K under high vacuum (1 mPa) for at least 8 h. As-synthesized samples containing crown ethers were evacuated at 393 K for at least 24 h. Micropore volumes were derived from the isotherms using the T-plot method of Lippens and de Boer.[29]

A CHEMX molecular graphics package from Chemical Design was used for evaluating the fitting of the Na–18-crown-6 complex in cavities of the EMT structure.

Procedures. Changes in the degree of crystallinity of the synthesized solids were followed with FT-IR. It is based on the intensity ratio of the 585-cm^{-1} band, assigned to a combination vibration mode of double six-rings,[30] and the 450-cm^{-1} band, attributed to the Si(Al)–O bending.[30] The former mode is structure sensitive and is only present when the

(26) Wiles, D. B.; Young, R. A. *J. Appl. Crystallogr.* **1981**, *14*, 149–151.
(27) Lievens, J. L.; Verduijn, J. P.; Bons, A. J.; Mortier, W. J. *Zeolites* **1992**, *12*, 698–705.
(28) Hill, R. J.; Howard, C. J. *J. Appl. Crystallogr.* **1987**, *20*, 467–474.
(29) Lippens, B. C.; de Boer, J. H. *J. Catal.* **1965**, *4*, 319–323.
(30) Flanigen, E. M.; Khatami, H.; Szymanski, H. A. *Adv. Chem. Ser.* **1971**, *101*, 201–229.

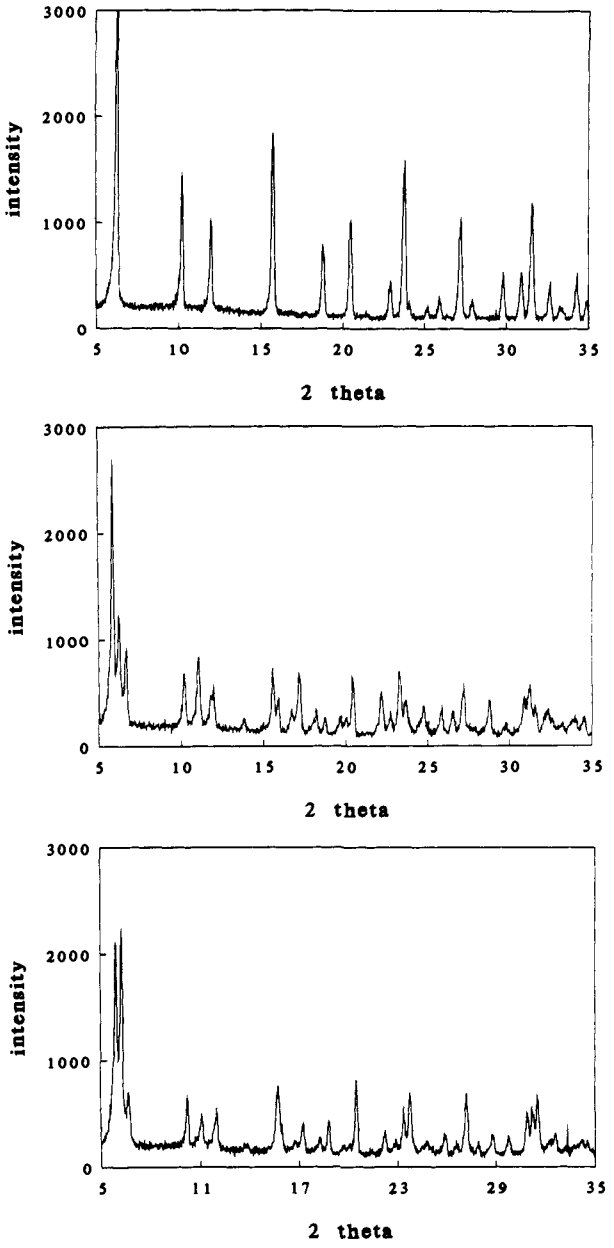

Figure 2. Powder X-ray diffraction patterns of the calcined samples, obtained after 9 days of crystallization: (a, top) FAU-15, (b, middle) EMT-18, (c, bottom) MIX 20/80.

sample contains double six-rings and thus crystalline material. The latter mode is a structure-insensitive vibration, which is also present in amorphous silica–alumina.

Nucleation curves during crystallization were determined as described by Zhdanov and Samulevich.[31,32] It consists of a combination of a size increase curve (of the largest crystal) in time and a histogram of crystal size distribution in the final product.

Results

The nature of the crystalline phases obtained after 9 days of crystallization was determined with XRD. Either FAU phases were obtained (samples FAU-0, FAU-15, FAU-18 a, b, c, and d, and MIX 60/40) or an EMT phase (EMT-18) or FAU/EMT polytype materials (MIX 40/60, 25/75, 20/80, 15/85, and 10/90) (Table 1). Powder XRD patterns of some of the crystallization products are shown in Figure 2. The intensity ratio of the vibration

(31) Zhdanov, S. P.; Samulevich, N. N. Proceedings of The Fifth International Conference on Zeolites; Rees, L. V., Ed.; Heyden: Chichester, 1980; pp 75–84.

(32) Barrer, R. M. *Hydrothermal Chemistry of Zeolites*; Academic Press: London, 1982; pp 145–151.

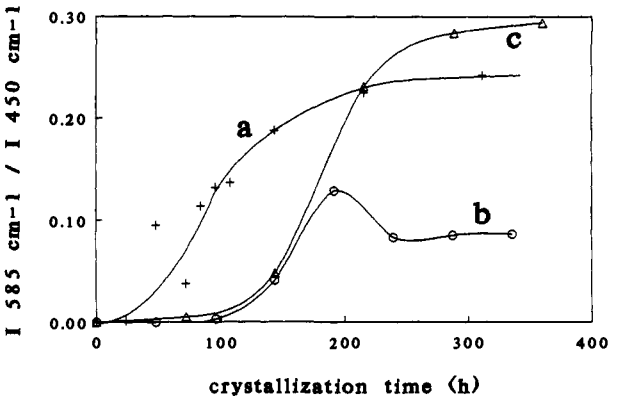

Figure 3. Crystallization curves for (a) EMT-18, (b) FAU-0, and (c) FAU-15.

of the double six-ring (585 cm^{-1}) and the Si(Al)–O bending (450 cm^{-1}) was used to measure the variation of the degree of crystallinity during the course of crystallization of FAU-0, EMT-18, and FAU-15 (Figure 3). The presence of 18-crown-6 ether in the gel induces a fast crystallization. The crystallization curve is delayed by ca. 75 h when synthesis occurs in the absence of 18-crown-6. In total absence of any crown ether, the sample does not reach high crystallinity. Scanning electron micrographs of typical crystals of FAU-15, EMT-18, and FAU-18b are displayed in Figure 4. FAU-15 and EMT-18 crystals have the typical cubic and hexagonal platelet morphology, respectively. The FAU-18b sample consists of spherical particles with irregular surface.

Nucleation curves determined via Zhdanov and Samulevich's method[31,32] are shown in Figure 5. The nucleation rate for the zeolites within the first 60 h is clearly non-zero, which seems in contradiction with IR-derived data in Figure 3. However, as zeolite nucleation unfortunately is beyond the detectibility limit of IR (and all other physicochemical methods), nucleation data are only accessible via indirect methods. The nucleation curves are derived from size increase curves of even a small number of large crystals, which are not necessarily physicochemically detectable.

Nucleation is found to be significantly faster in the presence of crown ethers in general, and more specifically in the presence of 18-crown-6 ether. Crystal growth rates were derived from the volumetric growth of the largest crystal in the batch using SEM data (Figure 6). The volumetric growth rate of EMT crystals in the presence of 18-crown-6 ether is 0.023 $\mu m^3\ h^{-1}$, compared to only 0.010 $\mu m^3\ h^{-1}$ for FAU crystals in the presence of 15-crown-5 ether and 0.002 $\mu m^3\ h^{-1}$ for FAU crystals in the absence of crown ethers.

The FAU and EMT content of the samples MIX 10/90, MIX 20/80, and MIX 40/60 obtained from Rietveld refinement of powder XRD patterns is given in Table 2. The EMT content is plotted against the molar 18-crown-6/(18-crown-6 + 15-crown-5) ether ratio in the gel ($\alpha_{18\text{-}c\text{-}6}$) in Figure 7. It follows that both parameters are related by the following equation:

$$\%\ \mathrm{EMT} = 2 \times [\alpha_{18\text{-}c\text{-}6} - 0.5] \times 100 \qquad (1)$$

with values for $\alpha_{18\text{-}c\text{-}6}$ within the range 0.50–1.00. Only from a critical 18-crown-6 ether fraction in the synthesis gel on can the EMT phase be detected in the crystalline product. For higher fractions, the EMT content in the crystal increases linearly with $\alpha_{18\text{-}c\text{-}6}$.

The micropore volume of dehydrated, as-synthesized and of calcined samples obtained after 9 days of crystallization is given in Table 3. All calcined products have a micropore volume exceeding 0.33 mL/g, which is indicative of a high degree of

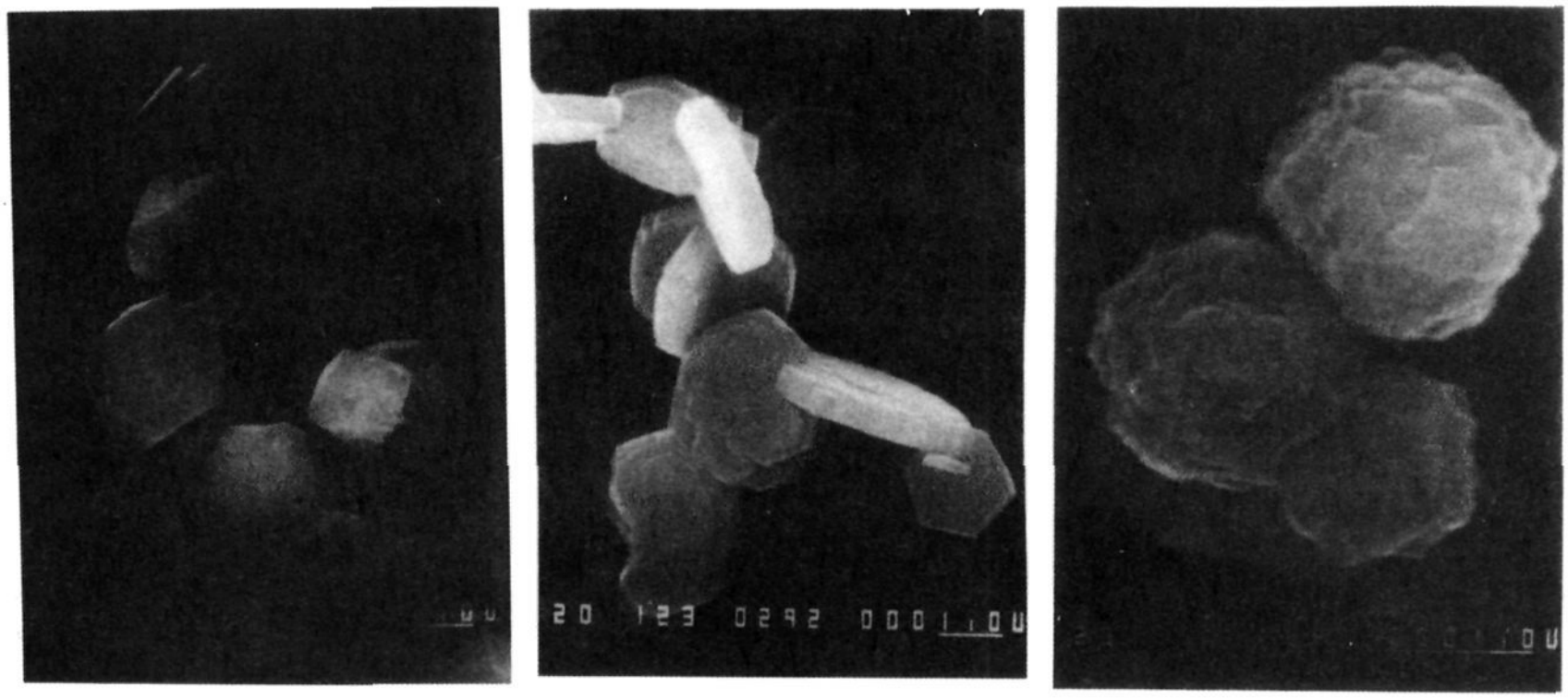

a b c

Figure 4. Scanning electron micrograph of crystals of (a) FAU-15, (b) EMT-18, and (c) FAU-18 b after 9 days of crystallization.

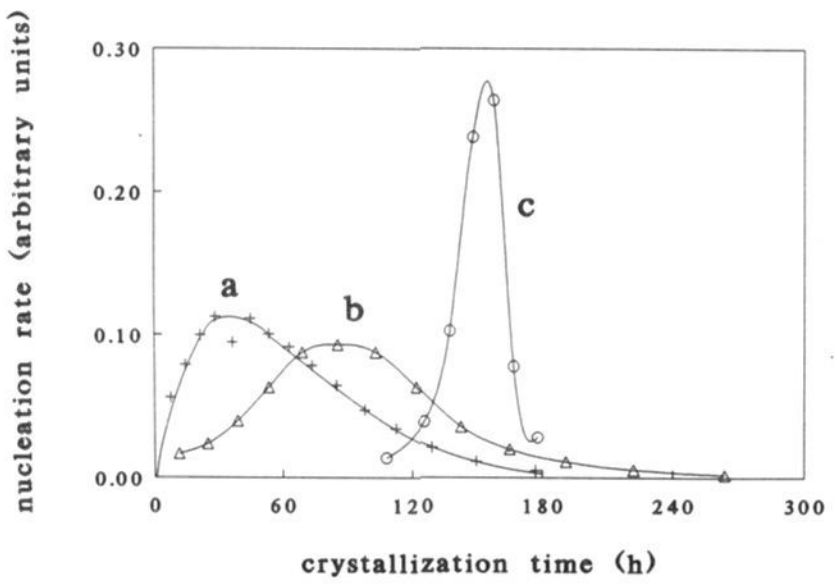

Figure 5. Nucleation rate curves for (a) EMT-18, (b) FAU-15, and (c) FAU-0.

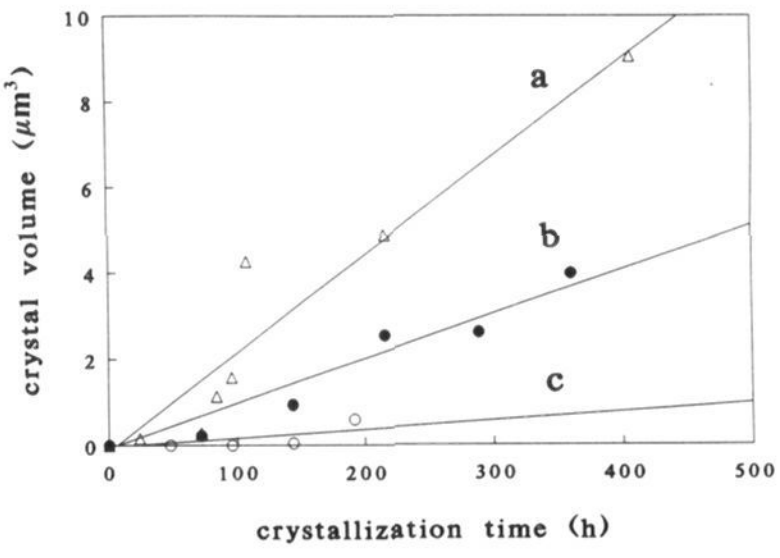

Figure 6. Crystal volume of the largest crystal versus crystallization time of (a) EMT-18, (b) FAU-15, and (c) FAU-0.

crystallinity.[33] In dehydrated, as-synthesized FAU samples containing 15-crown-5 or 18-crown-6 ether molecules (FAU-15, FAU-18 b-d), ca. 50% of the micropore volume is accessible toward nitrogen. The dehydrated, as-synthesized EMT-18 phase is devoid of any microporosity. Dehydrated uncalcined FAU/EMT polytype samples have a very small micropore volume, increasing slightly when the 15-crown-5 ether/18-crown-6 ether ratio in the gel is increased from 10/90 to 15/85 and 20/80.

(33) Lynch, J.; Raatz, F.; Dufresne, P. *Zeolites* **1987**, *7*, 333–340.

Table 2. EMT and FAU Content (%) in Intergrowths from Rietveld Refinement of XRD Powder Patterns

sample	% EMT	% FAU
MIX 10/90	82	18
MIX 20/80	56	44
MIX 40/60	8	92

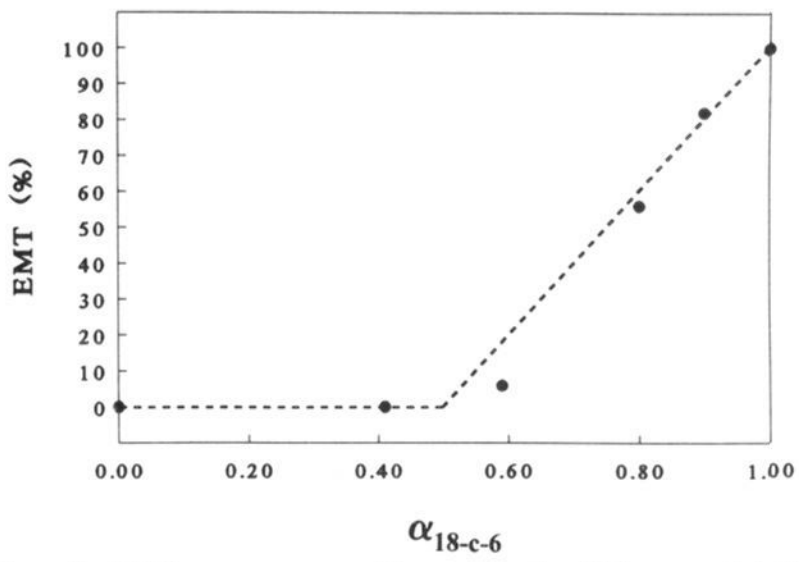

Figure 7. EMT content versus 18-crown-6 ether/(18-crown-6 + 15-crown-5 ether) molar ratio ($\alpha_{18\text{-c-}6}$) in the synthesis gel.

The ^{13}C CP NMR resonance envelope recorded under static conditions for an as-synthesized EMT-18 sample contains two discrete maxima at 79 and 66 ppm, respectively; as-synthesized FAU-15 shows only a single maximum at 68 ppm (Figure 8). For the as-synthesized sample MIX 20/80 the resonance line exhibits a shoulder around 66 ppm. These results confirm spectra reported earlier on similar samples.[24] Under MAS conditions, the splitting vanishes (Figure 9) and one line is observed for all samples. The chemical shifts of these lines can be found in Table 3. These values are in agreement with earlier work[17,24,34a] and point out that Na–crown ether complexes are present in the intracrystalline void space. The occurrence of line splitting only in EMT and EMT containing samples under static conditions is attributed to the existence of chemical shift anisotropy of EMT occluded 18-crown-6 ether molecules. It is straightforward to assign the 2 lines to different environments in EMT and therefore to 18-

(34) (a) Annen, M. J.; Young, D.; Arhancet, J. P.; Davis, M. E.; Schramm, S. *Zeolites* **1991**, *11*, 98–102. (b) Skeels, G. W.; Blackwell, C. S.; Reuter, K. B.; McGuire, N. K.; Bateman, C. A. In *Proceedings of the 9th International Zeolite Conference*, Montreal, 1992; von Balmoos, R., et al., Eds.; Butterworth-Heinemann, 1993.

Table 3. Micropore Volume, Lattice Si/Al Ratio, ^{13}C CP MAS NMR Chemical Shift, and Number of Crown Ethers per Unit Cell from TGA Profiles

sample notation	micropore volume (mL/g) as synthesized	micropore volume (mL/g) calcined	lattice Si/Al[d]	^{13}C NMR shift	crown ethers per unit cell
FAU			3.0		0.0
FAU-15	0.135		3.6	69.0	9.0
EMT-18	0.000	0.331	3.7	69.8	4.5
FAU-18 b	0.165	0.345	2.4	69.6	10.0
FAU-18 c	0.132	0.347	2.6		9.2
FAU-18 d	0.154		2.6		9.9
MIX 20/80	0.015	0.332	3.5	69.7	10.9[a,c]–9.1[b,c]
MIX 15/85	0.006	0.341		69.7	11.2[a,c]–9.3[b,c]
MIX 10/90	0.004	0.345		69.7	11.7[a,c]–9.7[b,c]

[a] Assuming 15-crown-5 is exclusively present. [b] Assuming 18-crown-6 is exclusively present. [c] Number of crown ethers per 192 T-atoms. [d] Derived from the ^{29}Si NMR spectra; for the faujasite polytypes, it is assumed that all peaks are within the FAU envelope.[34a,b]

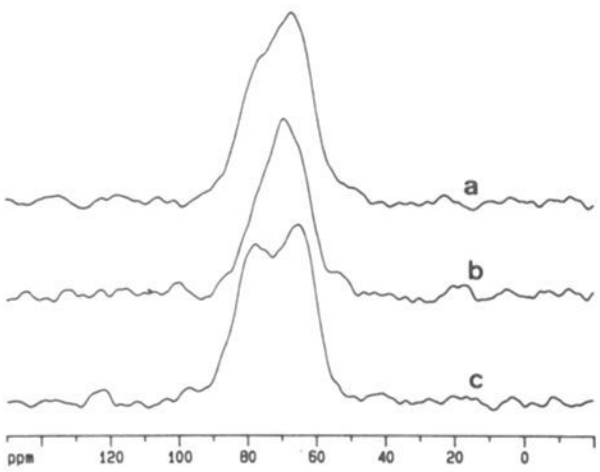

Figure 8. ^{13}C CP NMR spectra recorded under static conditions for dehydrated, as-synthesized samples of (a) MIX20/80, (b) FAU-15, and (c) EMT-18.

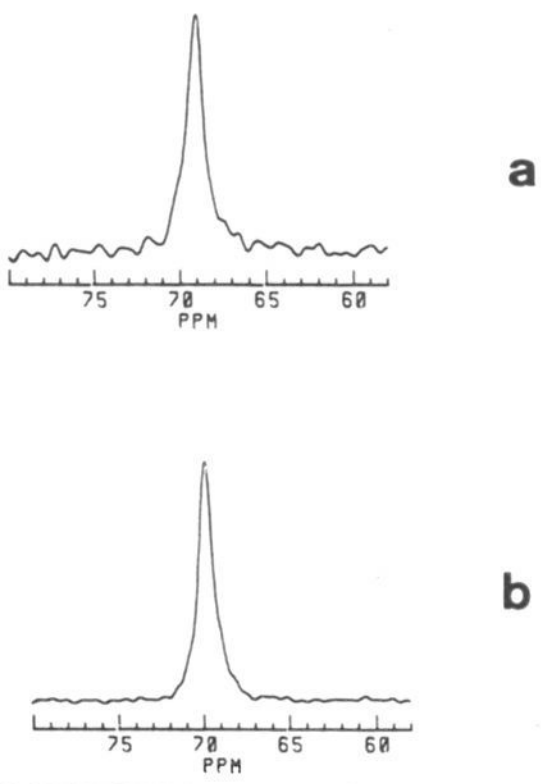

Figure 9. ^{13}C CP MAS NMR spectrum of as-synthesized (a) FAU-15 and (b) EMT-18.

crown-6 in hyper- and hypocages, respectively.

The number of crown ether molecules in the crystallization products was derived from the TGA profiles (Table 3). The FAU structure contains 8 supercages per unit cell. In the different syntheses where a FAU phase was obtained, the crown ether content varied between 9 and 10 crown ether molecules per unit cell. The EMT topology contains 2 hypocages and 2 hypercages per unit cell. The 18-crown-6 ether content of the EMT-18 sample corresponds to 4.5 molecules per unit cell. For the EMT/FAU polytype samples, the molar crown ether content cannot be derived exactly by TGA, since the ratio of the two crown ethers in the different samples is unknown. The values calculated for the number of crown ether molecules per 192 T-atoms in the MIX type of samples are similar to those found for the pure FAU and EMT samples (Table 3).

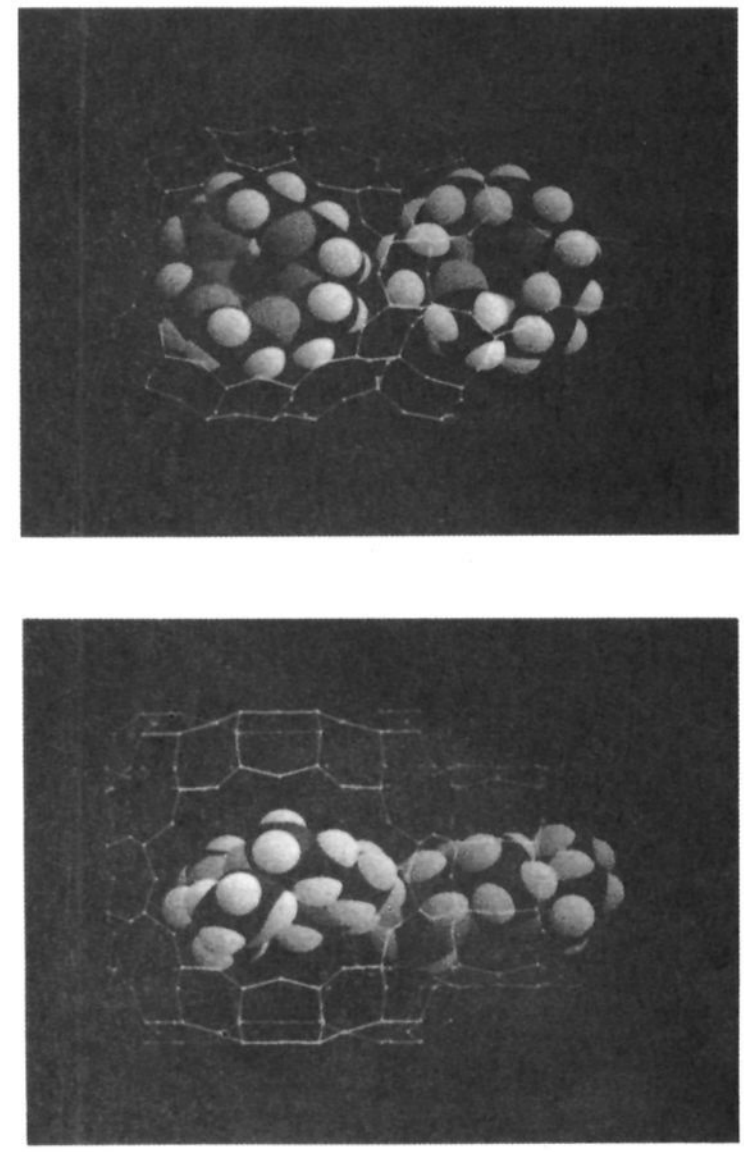

Figure 10. Molecular model of the Na–18-crown-6 ether complex in the hypocages and hypercages of the EMT framework: (a) view along the 001 direction; (b) view along the 100 direction.

The fitting of the Na–18-crown-6 ether complex in the hypocage and the hypercage was evaluated with molecular graphics (Figure 10). The coordinates for the Na–18-crown-6 ether complex and those for the hypo- and hypercage were derived from crystallographic data.[35,27] For this evaluation, silica frameworks with an atomic radius of 0.136 nm for oxygen and 0.026 nm for silicon were used. The values for the van der Waals radii of hydrogen, carbon, oxygen, and sodium in the Na–crown ether complexes were 0.100, 0.160, 0.136, and 0.098 nm, respectively. The van der Waals volume of the Na–18-crown-6 complex can be positioned inside the hypocage avoiding overlapping with the spheres representing the oxygen atoms in the walls of the cavity (Figure 10).

Discussion

Location of Crown Ether Molecules in Supercages, Hypocages, and Hypercages of FAU or EMT Topologies. For each of the FAU, EMT, and FAU/EMT polytype samples investigated, the crown ether content is sufficient to locate at least 1 crown ether molecule in each hypo-, super-, and hypercage (Table 3). In the molecular graphics picture of the hypocage encapsulated Na–18-crown-6 complex, very little free space is left in the hypocage, not even sufficient for locating a supplementary nitrogen molecule, or a hydrated sodium cation. If it is assumed that the hypocage is an ellipsoid with diameters of 0.69 nm × 1.3 nm × 1.3 nm, its void volume should correspond to 0.61 nm^3. The void volume of

(35) Dobler, M.; Dunitz, J. P.; Seiler, P. *Acta Crystallogr.* **1974**, *B30*, 2741–2743.

the supercage—a sphere with a radius of 1.3 nm—is substantially larger, viz. 1.15 nm^3. For the hypercage, represented as an ellipsoid of 1.3 nm × 1.3 nm × 1.4 nm, it is 1.24 nm^3. The hypercage is about twice as large as the hypocage and can easily accommodate a crown ether molecule (Figure 10). After filling a hypercage or supercage with a Na–crown ether complex, about half of the void volume is left vacant. This explains why the micropore volume of dehydrated, as-synthesized FAU samples containing 15-crown-5 ether (FAU-15) or 18-crown-6 ether (FAU-18 b-d) is about half of that of calcined samples (Table 3).

In the dehydrated, as-synthesized EMT-18 sample, it is estimated from the molecular model (Figure 10) that nitrogen adsorption is only possible in hypercages, since the hypocages are completely filled with Na–18-crown-6 complexes. However, if in the hypercages the 18-crown-6 ether molecules are oriented perpendicular to the *c* axis, as suggested by Delprato et al.,[17] the hypercage channels are blocked too, explaining the absence of any nitrogen adsorption capacity in the EMT-18 sample (Table 3). The presence of 1 crown ether molecule per cage is in agreement with results obtained by thermoanalysis on similar samples.[24,34a] Alternative siting patterns for the crown ethers suggested previously, e.g. hypocages devoid of 18-crown-6 ether molecules[17] or crown ethers located primarily in hypocages,[25] are inconsistent with the present nitrogen sorption data obtained on dehydrated, as-synthesized samples.

The FAU/EMT polytype materials (MIX 20/80, 15/85, and 10/90) show small micropore volumes (Table 3). In such materials, nitrogen sorption is only possible in the FAU regions which are accessible from the external crystal surface. FAU regions covered by an EMT layer are not accessible for nitrogen molecules. The as-synthesized sample MIX 20/80 contains 44% FAU (Table 2) as derived from Rietveld refinement of XRD patterns. Its micropore volume is ca. 10% of that of as-synthesized FAU samples, suggesting that ca. 10% of these crystals consist of accessible FAU domains, not surrounded by EMT layers. Thus, from the total number of FAU layers in the sample MIX 20/80, ca. 23% are accessible, while 77% are inaccessible. The sample MIX 10/90 contains 18% FAU (Table 2) and has a micropore volume of only 0.004 mL/g, which is ca. 3% of that of pure FAU samples (Table 3), indicating that ca. 3% of the sample consists of accessible FAU layers. From the total FAU content in the sample only 15% is accessible, while 85% is inaccessible. It is concluded that in intergrowths containing less FAU, the FAU domains on a relative basis are less accessible and/or the size of individual FAU layers must be smaller. Using high-resolution electron microscopy, Terasaki et al.[25] investigated a FAU/EMT sample, prepared from a gel containing a mixture of crown ethers. They found that the two types of phases were present as perfectly intergrown structures. Individual blocks of FAU and EMT a few unit cells thick are stacked in the direction corresponding to the 111_{CUBIC} and 001_{HEX} axes. The present data strongly suggest that the presence of alternating layers of FAU and EMT in intergrown samples with EMT/FAU topology is a general property of such materials.

Role of Crown Ether Molecules during Crystal Growth. The role of cations in the synthesis mechanism of FAU and EMT zeolites can be qualitatively understood in terms of Vaughan's "extended structure approach".[36] Primary cations (hydrated Na^+ in the present case) determine the generation of the important structure building units. In the FAU/EMT case, these building units are probably formed by *faujasite layers* consisting of a sheet of cubo-octahedra interconnected through hexagonal prisms.[36] When *faujasite layers* are assembled with the help of secondary cations in such a way that the second layer is the mirror image of the first one, the EMT topology is generated. As there exist three inequivalent relative positions for such 2 layers, denoted as A, B, and C, a stacking sequence of individual cubo-octahedra in adjoining layers can be ABABAB or ABCABC. The first sequence is encountered in the EMT topology (Figure 1), while in the second one the positions of pairs of cubo-octahedra in adjoining layers are related to each other via an inversion center. The latter arrangement of cubo-octahedra is encountered in the FAU topology (Figure 1).

In the synthesis of faujasites, Na^+ acts as the primary cation. The presence of hydrated Li^+ or Cs^+ in the hydrogel introduces a certain amount of hexagonal instead of cubic stacking of the sheets.[10,11,20] In the absence of secondary cations or in the presence of cations with a weak secondary impact, the synthesis proceeds toward the structure characteristic of the primary cation, which is FAU in this instance.

Following the extended structure approach of crown ether mediated syntheses, hydrated Na^+ cations must be regarded as the primary cations, while the Na–crown ether complexes function as secondary cations and are responsible for the linking of the sheets according to the hexagonal (Na–18-crown-6 ether) or cubic symmetry (Na–15-crown-5 ether). Therefore, the primary/secondary cation ratio in the gel should be the principal synthesis parameter determining the outcome of the crystallization.

In the present work, a pure EMT phase was obtained when the 18-crown-6 ether/Na_2O ratio in the gel was 0.405 (Table 1, sample EMT-18). When this ratio was decreased to values of 0.324 and 0.258, pure FAU instead of EMT phases were crystallized (Table 1, sample FAU-18 a and b, respectively), in agreement with the model. However, in another synthesis with a 18-crown-6 ether/Na_2O ratio of 0.405, the Na_2O/SiO_2 as well as the OH^-/SiO_2 ratio was increased. As a pure FAU phase was obtained (Table 1, sample FAU-18 c), this result shows that the structure directing role exerted by Na–18-crown-6 ether complexes is lost in conditions of high alkalinity or in the presence of increased Na_2O/SiO_2 and/or OH^-/SiO_2 ratios in the gel. A similar observation has been made by Burkett and Davis.[24] For the synthesis of sample FAU-18 d, only the Na_2O/SiO_2 ratio was increased without altering the OH^-/SiO_2 ratio through the use of sodium aluminate instead of Gibbsite as the source of aluminum. The FAU nature of the phase obtained in this experiment suggests that the Na_2O/SiO_2 rather than the OH^-/SiO_2 ratio is of critical importance.

The use of an enhanced Na_2O/SiO_2 ratio in the gel irrespective of the values for the OH^-/SiO_2 or 18-crown-6 ether/Na_2O ratios invariably leads to aluminum-enriched frameworks (Table 3). Barrer reported as similar influence of the Na_2O/SiO_2 ratio on the Si/Al ratio of a zeolite A product, crystallized from hydrogels prepared with various proportions of NaOH and tetramethylammonium hydroxide.[37]

Terasaki et al. observed that the growth of EMT crystals in the presence of 18-crown-6 ether is strongly anisotropic.[25] The growth rate in 001_{HEX} planes is ca. 15 times faster than in 100_{HEX} and 010_{HEX} planes. Observation of the crystal growth pattern with high-resolution electron microscopy led them to conclude that EMT crystals grow by addition in the 001_{HEX} direction of layers that are half a unit cell thick, thus corresponding to a faujasite sheet. Burkett and Davis arrived at the same conclusion based on the impact of systematic variations of synthesis conditions on the outcome of the crystallization.[24] They concluded that the presence of Na–18-crown-6 ether complexes in the hypocages is essential to the synthesis of EMT.[24]

A hypothetical surface of a growing faujasite polytype crystal is schematically represented in Figure 12. The crystal is terminated by a faujasite layer consisting of sodalite cages, connected through hexagonal prisms. For crystals with FAU topology, 8 equivalent faces having this surface structure are available in the $[111]_{CUBIC}$ direction. In crystals of EMT, the

(36) Vaughan, D. E. W. *Catalysis and Adsorption by Zeolites*; Ohlmann, G., Pfeifer, H., Fricke, R., Eds.; Elsevier: Amsterdam, 1991; pp 275–286.

(37) Barrer, R. M. *Hydrothermal Chemistry of Zeolites*; Academic Press: London, 1982; p 160.

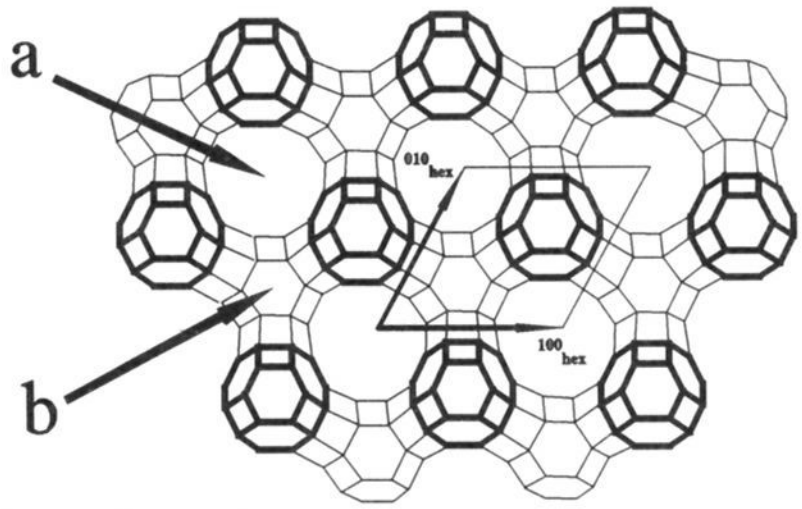

Figure 11. Line drawing of a faujasite sheet, showing the connectivity of sodalite cages and the presence of hyperholes (a) and hypoholes (b).

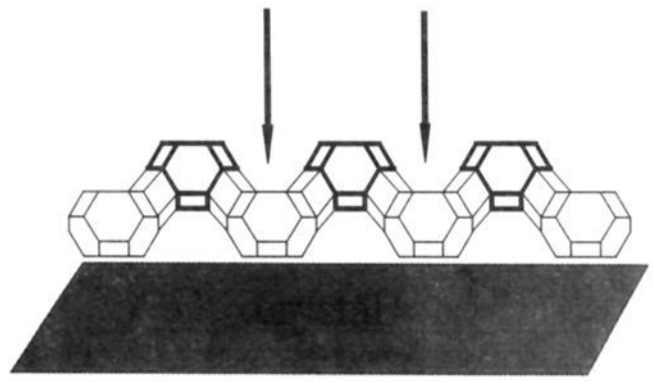

Figure 12. Line drawing of an hypothetical framework termination at $[111]_{CUBIC}$ and 001_{HEX} faces of a growing faujasite crystal. Arrows locate the holes in which Na–crown ether complexes are sited.

surface structure shown in Figure 12 occurs perpendicular to the 001_{HEX} direction. In this hypothetical surface, two types of holes are present that will further be referred to as "hypohole" and "hyperhole", respectively (Figures 11 and 12). During crystal growth, the surface transforms into a FAU or EMT, depending on the relative position of the new layer(s) added on top of it. If crystal growth proceeds according to the EMT mode, hypoholes and hyperholes develop into hypocages and hypercages, respectively. Alternatively, when the new layer is added so that FAU topology is adopted, both types of holes are transformed into supercages. The present data do not give information on the size of such layers. Terasaki et al.[25] revealed that the 001_{HEX} planes start to grow from the central axis of the crystal, subsequent faces beginning to appear when *ca.* 30 unit cells of these planes are completed in the $010_{HEX}/100_{HEX}$ directions. More work is needed, however, to confirm that such dimensions are relevant for faujasite layers in synthesis conditions.

Since 18-crown-6 ether molecules for steric reasons are excluded from calcined FAU and EMT structures,[24] they must be encapsulated in the cages during the crystal growth process. Consequently, the present sorption results on as-synthesized samples indicate that crystal growth requires a full occupation of the hypo- and hyperholes with Na–18-crown-6 ether complexes. Molecular graphics suggest that only in hypocages is a tight fit of the Na–18-crown-6 complex with structure elements possible. This favorable interaction of the Na–18-crown-6 complex with the hypocage suggests that this complex exerts a structuring role. The molecular graphics model suggests that crown ethers should have less structuring potential for supercage and hypercage formation. Thus, occupation of hypoholes by Na–18-crown-6 ether complexes is expected to favor the conversion of a hypohole into a hypocage rather than into a supercage and the addition of the new faujasite top layer according to the hexagonal stacking mode.

The Na–18-crown-6 ether complex is a monovalent macrocation capable of neutralizing only one negative charge of the zeolite surface. If the number of negative charges to be neutralized in the hypohole is larger, additional Na^+ cations must necessarily be occluded together with the complex, and hypocage formation for sterical reasons is inhibited. In such an instance, the hypohole has to be converted into a larger cage, the supercage of the FAU structure being the only available alternative. This model requires the existence of a lower limit for the framework Si/Al ratio in EMT phases crystallized in the presence of 18-crown-6 ether. This limiting value should be located between Si/Al ratios of 3.7 and 2.6. Indeed, Table 3 shows that a pure EMT phase with a Si/Al ratio of 3.7 easily crystallizes, while for decreased Si/Al ratios of the hydrogel (Table 1) EMT no longer crystallizes if the Si/Al ratios of the products are 2.6 or less.

The observations made in synthesis using mixtures of 18-crown-6 and 15-crown-5 ethers are also consistent with crystal growth involving crown ether deposition in hypoholes and hyperholes. During crystal growth, Na complexes of the two types of crown ethers should compete for the hypo- and hyperholes on the crystal surface. Nucleation as well as growth of EMT crystals in presence of 18-crown-6 ether is substantially faster than that of FAU crystals in the presence of 15-crown-5 or of Na^+ cations. This result suggests that the formation of hypocages with occluded 18-crown-6 ether is faster than that of supercages with occluded 15-crown-5 ether. The absence of EMT formation when 18-crown-6 ether molecules are present in minority (Figure 7) is then interpreted by Na–18-crown-6 complexes being deposited selectively in hyperholes, where they do not exert a structure directing function. EMT formation sets in provided hypoholes are present containing a Na–18-crown-6 complex, i.e. only in the presence of excess 18-crown-6 ether. The growth of EMT layers consumes selectively 18-crown-6 ether, since hypercages as well as hypocages are filled preferentially with Na–18-crown-6 ether complex. Growth of EMT continues until the 18-crown-6/15-crown-5 ether concentration ratio in the vicinity of the growing crystal is decreased below the critical value. Crystal growth switches then to the FAU mode until the critical 18-crown-6/15-crown-5 ether concentration ratio is restored again. The intergrown nature of the mixed faujasite samples with the frequent alternation of FAU and EMT layers and the relationship of EMT content with crown ether composition (eq 1) is understood in the light of such a mechanism. The proposed growth pattern involves the following occupation of the cavities with crown ether: hypocages and hypercages contain essentially 18-crown-6 ether, supercages can contain either a 15-crown-5 or an 18-crown-6 ether molecule. The correlation between selectivity for EMT and the presence of 18-crown-6 ether in the hydrogel for systems containing also 15-crown-5 ether seems less strict than predicted by molecular graphics. Indeed, an 18-crown-6 ether fraction of at least 0.5 is required to stimulate EMT growth. Therefore, in the holes of growing crystal planes decorated with lattice terminating hydroxyl groups, the fit of 18-crown-6 in hypoholes for obvious steric reasons seems less perfect, probably resulting in the formation of 15-crown-5 filled hypoholes, alternating with 18-crown-6 filled hyperholes, thus failing to template EMT for 18-crown-6 fractions below 0.5. For higher values, 18-crown-6 will be accommodated again in the hypoholes and template EMT formation. The crystallization of crown ether containing faujasites is a first clear example of self-assembling of organic and inorganic macromolecules during crystal growth of a zeolite.

Conclusions

On the basis of ^{13}C CP MAS NMR, TGA, and nitrogen adsorption at 77 K, it is derived that in pure FAU and EMT topologies as well as in FAU/EMT intergrowths each type of cage contains one Na–crown ether complex. These complexes are occluded in the zeolite during crystal growth. The rate of nucleation and growth of EMT crystals in the presence of 18-crown-6 ether is faster than that of FAU crystals in the presence of 15-crown-5 ether and from inorganic gels. Crystal growth in the presence of 18-crown-6 ether involves addition of single

faujasite layers on 001_{HEX} and 111_{CUBIC} surfaces. The growth of EMT requires (i) the presence of Na–18-crown-6 ether complexes in the hypoholes of the growing surface (this requires a minimum fraction of 18-crown-6 of 0.5 for synthesis of faujasite intergrowths by using a mixture of 18-crown-6 and 15-crown-5) and (ii) a sufficiently low Na_2O/SiO_2 ratio to obtain a low lattice Al content, not necessitating the incorporation of supplementary sodium cations for charge compensation in hypocages. In gels containing only 18-crown-6, this condition is met at a Na_2O/SiO_2 ratio of 0.24. Higher Na contents of the gel necessarily lead to aluminum-enriched frameworks of the FAU type.

The EMT content of FAU/EMT intergrowths crystallized in the presence of a mixture of 18-crown-6 and 15-crown-5 ether is correlated linearly to the 18-crown-6 fraction, starting from a critical value of 50% of 18-crown-6. Na–18-crown-6 ether complexes are preferentially occupying hyperholes, where they do not exert a structure directing function. An excess of 18-crown-6 ether is required to fill hypoholes with the Na–18-crown-6 ether complex and to provoke growth of EMT. EMT growth selectively consumes 18-crown-6 ether. Local exhaustion of 18-crown-6 causes a change of crystal growth from the EMT to the FAU topology until the critical crown ether composition required for EMT growth is restored. The model predicts that in FAU/EMT intergrowths obtained in the mixed crown ether system, hypocages and hypercages contain preferentially 18-crown-6 and that supercages can contain 18-crown-6 as well as 15-crown-5 ether. The crown ether molecule–faujasite sheet interaction is a clear example of a self-assembly mechanism of organic and inorganic macromolecules during a templated zeolite synthesis.

Acknowledgment. The authors acknowledge sponsoring in the form of a IUAP-PAI Federal Programme and from the Flemish NFWO. E.J.P.F. acknowledges the Belgian IWONL for a Research Grant and J.A.M. and P.J.G. the Flemish NFWO for a position as Senior Research Associate. The authors are indebted to H. Geerts and R. Reynders for obtaining the NMR spectra.